5.0 kV BREAKDOWN-VOLTAGE VERTICAL GaN p-n JUNCTION DIODES

Hayashi, Kentaro / Mishima, Tomoyoshi / Yoshino, Michitaka / Horikiri, Fumimasa / Ohta, Hiroshi

(出版者 / Publisher)
法政大学イオンビーム工学研究所

(雑誌名 / Journal or Publication Title)
PROCEEDINGS OF THE 36th SYMPOSIUM ON MATERIALS SCIENCE AND ENGINEERING RESEARCH CENTER OF ION BEAM TECHNOLOGY HOSEI UNIVERSITY (December 13, 2017)

(巻 / Volume)
36

(開始ページ / Start Page)
33

(終了ページ / End Page)
38

(発行年 / Year)
2018-02

(URL)
https://doi.org/10.15002/00030357

5.0 kV BREAKDOWN-VOLTAGE VERTICAL GaN p-n JUNCTION DIODES

Hiroshi Ohta[1], Kentaro Hayashi[1], Fumimasa Horikiri[2], Michitaka Yoshino[1], and Tomoyoshi Mishima[1]

[1] *Hosei University, 3-11-15 Midori-cho Koganei-si, Tokyo 184-0003, Japan*
[2] *Sciocs Company, Ltd. 880 Isagozawa-cho, Hitachi-si, Ibaraki 319-1418, Japan*

A high breakdown voltage of 5.0 kV has been achieved for the first time in vertical GaN p-n junction diodes by our newly developed guard-ring structures. Resistance device was inserted between the main diode portion and the guard-ring portion in a ring shaped p-n diode to generate a voltage drop over the resistance device by leakage current flowing the guard-ring portion under negatively biased conditions before the breakdown. The voltage at the outer mesa edge of the guard ring portion where the electric field intensity become highest and the destructive breakdown usually occurs decreases by the voltage drop occurs, so that the electric field concentration in the portion has been relaxed. By adopting this structure, the breakdown voltage (V_B) has been raised by a few hundred volts. With combining a measured low on-resistance (R_{on}) of 1.25 mΩcm^2, Baliga's figure of merit (V_B^2/R_{on}) was as high as 20 GW/cm^2.

I. Introduction

Since gallium nitride (GaN) has excellent properties such as a wide band gap, a high breakdown electric field, and a high saturation velocity, it is strongly expected to be applied to high power, high frequency and high temperature devices [1-4]. In recent years it has been possible to fabricate high quality freestanding GaN substrates, which has enabled to grow high quality GaN epitaxial layers on the substrates. This homo-epitaxial growth has dramatically improved in GaN device performances by introducing vertical device structures. By these properties, great attentions have been paid for GaN in applications to highly efficient power devices. GaN diodes and transistors with high breakdown voltages have been extensively reported by many researchers [5-26]. Previously, we realized a device with the high breakdown voltage (V_B) of 4.7 kV by field plate structures and insertion of low donor-concentration n-GaN layers on top of the drift layer in GaN p-n diodes on high quality free-standing substrates [6]. In most cases, however, the destruction occurs at the mesa edge of the diodes, and it seems that relaxation of the electric field concentration in this portion is insufficient. For the further increment of V_B, we have developed guard-ring structure p-n junction diodes [26-27]. In addition, the validity of the guard ring structure for the improvement of breakdown voltage was confirmed both by simulation of electric field distributions and by voltage drop measurements between the guard ring and the main diode.

II. Device Structure and Fabrication Process

The electric field intensities at the mesa edge of the diodes under reverse-biased conditions were simulated for a conventional circular diode and a circular diode surrounded with a ring shaped diode. For the latter case, anode electrodes of the circular portion and the ring potion were electrically connected by a common field-plate electrode. Figure 1 shows the simulated results of the electric field intensity distribution when the reverse voltage 5kV is applied to the ring shaped p-n diode. The same layer structure and the design rule as the measured sample were applied to the simulation. The electric field intensity at the outer mesa edge of the ring shaped portion is higher than the electric field intensity of the mesa edge of the circular potion. Addition of the ring shaped portion brought little advantage in V_B; hence the breakdown would occur at the ring. By the basis of these simulations, the following diodes have been considered.

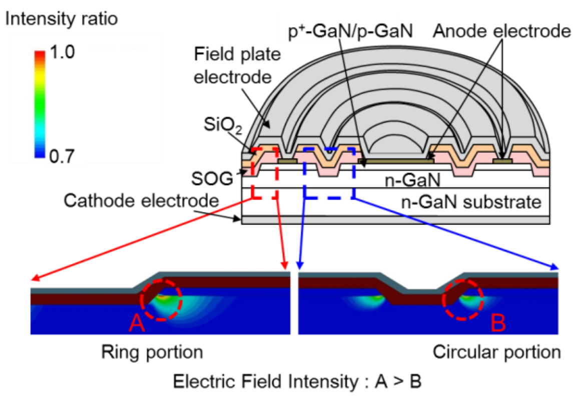

Fig. 1. Simulation result of electric field distribution at mesa edge of the p-n diode with a connected outer ring.

Figure 2 shows the schematic structure of the guard ring structure p-n diode newly proposed in this study. The guard-ring portion was placed around the main p-n diode portion, and a ring resistance device was inserted between the guard-ring portion and the main p-n diode portion. Figure 3 shows detailed illustration of the guard ring structure. When the reverse voltage is applied between the cathode electrode and the main diode portion in the guard ring structure p-n diode, a voltage drop V_d is generated between the main diode portion and the guard ring portion. V_d is expressed as $V_d = I \times R$ by the leakage current I flowing in the guard ring portion when the reverse voltage V is applied and the resistance value R of the resistance device at that time. The breakdown voltage of the outer mesa edge of the guard ring portion is defined as V_{b1}, and the breakdown voltage of the mesa edge of the main diode portion is defined as V_{b2}. When the reverse voltage $V = V_{b2}$ is applied between the cathode electrode and the main diode

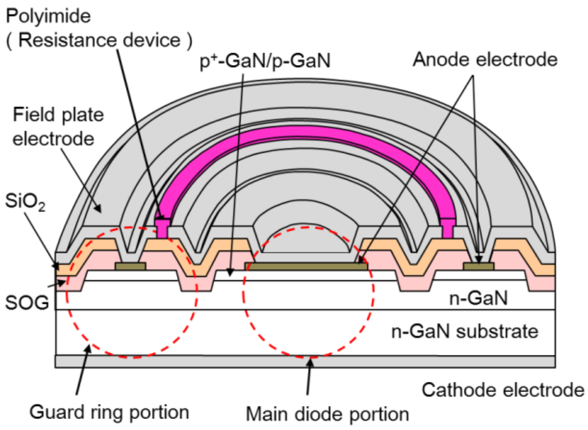

Fig. 2. Schematic cross section of guard ring structure p-n diode.

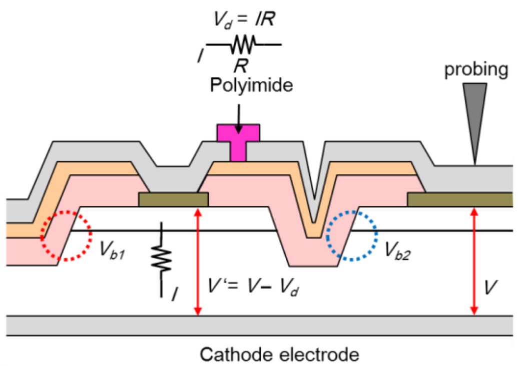

Fig. 3. Detailed illustration of the guard ring structure.

portion, destruction will occur at the main diode portion under the relation of $V_{b2} – V_{b1} < V_d$, in other words, the voltage at the guard ring portion $V_{b2} – V_d$ is smaller than V_{b1}. Therefore, by inserting the resistance that generates $V_d > V_{b2} – V_{b1}$, it is possible to expect an improvement in the breakdown voltage by $V_{b2} – V_{b1}$.

The layer structure shown in Figure 2 was grown by metal-organic vapor phase epitaxy (MO-VPE) on a free-standing GaN substrate fabricated by the void-assisted separation method with threading dislocation densities less than 3 x 10^6 cm^{-2} [28-29]. The epitaxial layers consist of p^+-GaN (Mg: 2 x $10^{20}/cm^3$, 30 nm)/p-GaN (Mg: 1 x $10^{18}/cm^3$, 500 nm)/ un-GaN (Si: < 2 x $10^{15}/cm^3$, 5.5 μm)/n^--GaN (Si: 9 x $10^{15}/cm^3$, 22 μm)/n^--GaN (Si: 1.6 x $10^{16}/cm^3$, 5.5 μm)/n-GaN (Si: 2 x $10^{18}/cm^3$, 2 μm) on a GaN substrate (n = 2 x $10^{18}/cm^3$, 400 μm). This structure is the same as that we previously achieved 4.7 kV breakdown voltages [6]. After the MO-VPE growth, thermal annealing was performed at 850 ºC for 30 minutes under N_2 ambient in order to activate Mg acceptors by removing adherent hydrogen atoms. The mesa structure was fabricated by inductively coupled plasma (ICP) dry etching using Ar and CF_4. In our previous study [6], the mask for mesa etching used a single-layer Ni mask, but in this study, the mask for mesa etching had a thick three-layer structure of Spin-on-Glass (SOG) / SiO2 / Ni (400/200/300 nm). Other fabrication procedure of our conventional diode structures has been mentioned in detail elsewhere [5]. Photosensitive polyimide (HD8820 manufactured by Hitachi Chemical Co., Ltd.) was used for resistance devices inserted between the guard-ring portion and the main p-n diode portion. The width of the resistance device was set to 4 μm. After pattern formation by conventional lithography, the polyimide was baked at 350 ºC for 30 minutes under air to cure. The diameter of the circular Pd non-alloy ohmic electrode was 60 μm. Current-voltage (I-V) characteristic were evaluated using Agilent B1505A combined with an ultra-high-voltage unit at room temperature while measured chips were immersed in insulating oil.

III. Results and Discussion

Prior to the evaluation of the characteristics of the diode, the value of the voltage drop generated in the polyimide was evaluated using the device shown in Fig. 4. It is characterized in that contact hole is not formed on the main diode portion and electrically insulated from the field plate electrode. By comparing the breakdown voltage of the diode with the width of the polyimide, it is possible to estimate the voltage drop. Figure 5 shows the voltage drop measurement results. In this figure, 0 on the horizontal axis corresponds to the structure of the polyimide being not inserted. It can be seen that the breakdown voltage has increased by about 0.2 to 0.4 kV. This

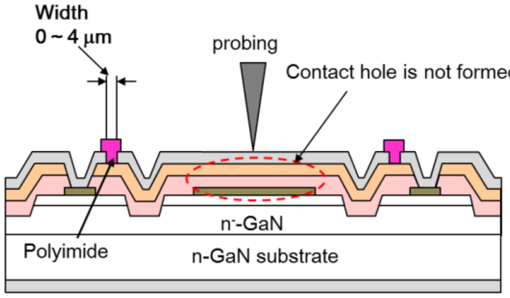

Fig. 4. Cross section of the device for the evaluation for the voltage drop at the polyimide.

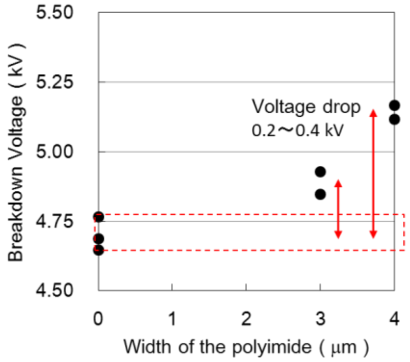

Fig. 5. Measurement results of voltage drop.

increment was caused by the voltage drop V_d generated at the polyimide. The resistance value of the polyimide varied by the applied voltages. It was estimated to be about 10 GΩ by the measured leakage current at the applied voltage of 0.2 to 0.4 kV between the anode electrode of the main diode and the ring diode portion.

Figure 6 shows the forward I-V characteristics of guard-ring structure p-n diode and normal circular p-n diode. For measurement, the polyimide having a width of 4 μm was used in the guard-ring structure p-n diode. In the former diode, the on-resistance (R_{on}) was 1.25 mΩcm^2 at forward voltage 5 V. R_{on} was calculated with the area of the main diode portions. The value was almost the same as R_{on} of the latter diode. Since a high resistance polyimide was inserted between the guard-ring portion and the main p-n diode portion, the guard-ring portion did not contribute to the forward current. In this study, since the three-layer structure was used as the mask for mesa etching, it became possible to avoid ion-irradiation damage to the p-GaN layer through the mask. Therefore, R_{on} could be lower than previous process using the single-layer Ni mask.

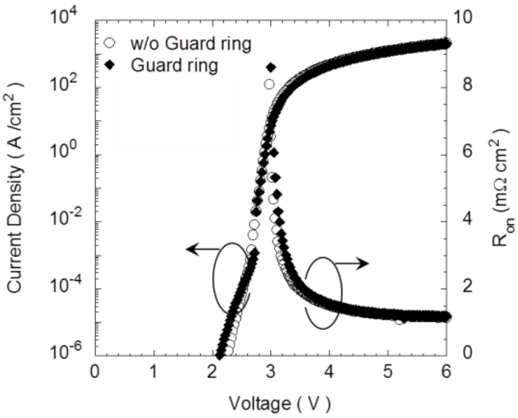

Fig. 6. Forward I-V characteristics of guard ring structure p-n diode.

Figure 7 shows the reverse I-V characteristics of guard-ring structure p-n diode and normal circular p-n diode. In the guard-ring structure p-n diode, the breakdown voltage (V_B) was 5.0 kV which was about 0.2 kV higher than 4.8 kV of the normal circular p-n diode. The V_B of 5.0 kV is the highest among so-far reported V_B of the vertical structure GaN p-n diodes. The Baliga's figure of merit (V_{B2}/R_{on}) [30] in this study was 20 GW/cm^2.

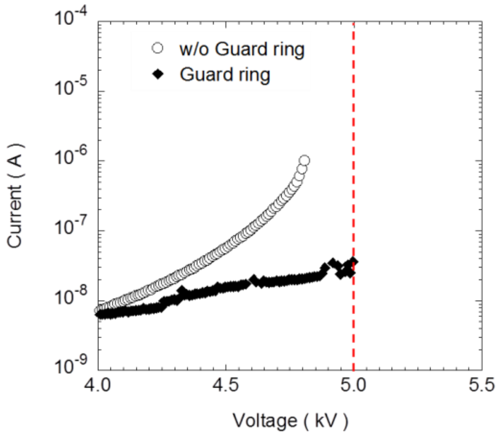

Fig. 7. Reverse I-V characteristics of guard ring structure p-n diode.

Figure 8 shows the surface of the guard-ring structure diode after the V_B measurement. The diode was destroyed at the mesa edge of the main diode portion as expected by the description at Fig. 3.

Since the breakdown occurred at the mesa edge of the main diode, V_{b2} in this device could be considered to be 5.0 kV. On the other hand, since V_B of the normal circular p-n diode was 4.8 kV, V_{b1} would be 4.8 kV. The increment value of 0.2 kV ($=V_{b2} - V_{b1}$) was less than the measured voltage drop V_d (0.4 kV) by polyimide. Therefore, the formula of $V_d > V_{b2} - V_{b1}$ has been satisfied in this device and there has been more room for the improvement in V_B.

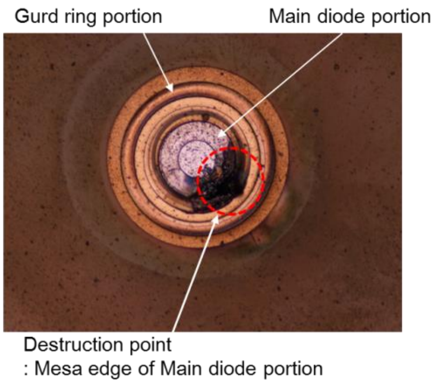

Fig. 8. Surface of the broken diode by 5.0 kV bias.

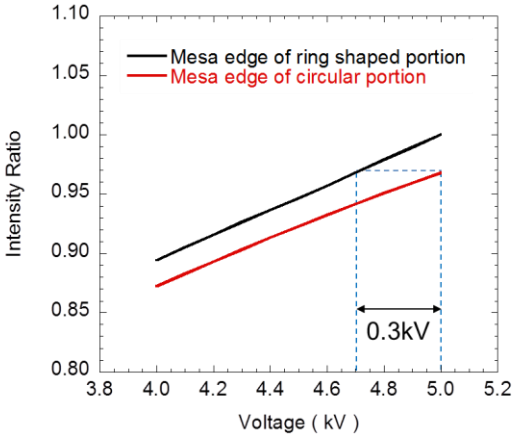

Fig. 9. Simulation results of electric field intensity dependence on reverse voltage.

Figure 9 shows the simulation results of electric field intensity dependence on voltage for the ring shaped p-n diode. The electric field intensity of the circular diode portion at the applied voltage of 5.0 kV was equal to that of the ring shaped portion at 4.7 kV. The discrepancy (0.3 kV) is close to the measured breakdown voltage improvement of 0.2 kV. This simulation has supported the above discussions.

IV. Conclusions

In order to increase the V_B of the p-n diodes, we developed guard-ring structure p-n diodes in which resistance devices were inserted between the guard-ring portion and the main p-n diode portion. In the guard-ring structure p-n diode, the breakdown voltage was 5.0 kV which was about 0.2 kV higher than 4.8 kV of the normal circular p-n diode. This increment was lower than the voltage drop of the resistance device and there would be more room for the improvement. The Baliga's figure of merit resulted in this study was as high as 20 GW/cm^2.

Acknowledgments
The authors thank the Japan Ministry of the Environment for their support.

References

1) A. M. Ozbek and B. J. Baliga, IEEE Electron Device Lett. 32, 300 (2011).
2) Y. Oshima, T. Yoshida, T. Eri, M. Shibata, and T. Mishima, Phys. Status Solidi C 4, 2215 (2007).
3) R. B. Simon, J. Anaya, and M. Kuball, Appl. Phys. Lett. 105, 202105-1 (2014).
4) C. Mion, J. F. Muth, E. A. Preble, and D. Hanser, Appl. Phys. Lett. 89, 092123-1 (2006).
5) Y. Hatakeyama, K. Nomoto, A. Terano, N. Kaneda, T.Tsuchiya, T. Mishima, and T. Nakamura, Jpn. J. Appl. Phys. 52, 028007-1 (2013).
6) H. Ohta, N. Kaneda, F. Horikiri, Y. Narita, T. Yoshida, T.Mishima, and T. Nakamura, IEEE Electron Device Lett. 36, 1180 (2015).
7) H. Ohta, F. Horikiri, Tohru Nakamura, Tomoyoshi Mishima, Nuclear Instruments and Methods in Physics Research B 409, 65, (2017).

8) I. C. Kizilyalli, T. Prunty, and O. Aktas, IEEE Electron Devices Lett. 36, 1073 (2015).
9) K. Nomoto, Y. Hatakeyama, H. Katayose, N. Kaneda, T. Mishima, and T. Nakamura, Phys. Stat. Sol. A 208, 1535 (2011).
10) Y. Hatakeyama, K. Nomoto, N. Kaneda, T. Mishima, and T. Nakamura, IEEE Electron Device Lett. 32, 1674 (2011).
11) T. Oka, Y. Ueno, T. Ina, and K. Hasegawa, Appl. Phys. Exp. 7, 021002 (2014).
12) D. Disney, H. Nie, A. Edwards, D. Bour, H. Shah, and I. C. Kizilyalli, in Proc. IEEE Int. Symp. Power Semicond. Devices ICs (ISPSD) (Kanazawa, Japan), 59 (2013).
13) B. Lu and T. Palacios, IEEE Electron Device Lett. 31, 951 (2010).
14) I. C. Kizilyalli, A. P. Edwards, H. Nie, D. Disney, and D. Bour, IEEE Trans. Electron Devices 60, 3067 (2013).
15) Y. Yoshizumi, S. Hashimoto, T. Tanabe, and M. Kiyama, J. Cryst. Growth 298, 875 (2007).
16) J. B. Limb, D. Yoo, J.-H. Ryou, W. Lee, S.-C. Shen, and R. D. Dupui, Electron. Lett. 42, 1313 (2006).
17) K. Nomoto, T. Nakamura, N. Kaneda, T. Kawano, T. Tsuchiya, and T. Mishima, Intl. Conf. Silicon Carbide and Related Materials, We-P-76 (2011).
18) I. C. Kizilyalli, A. P. Edwards, H. Nie, D. Bour, T. Prunty, and D. Disney, IEEE Electron Device Lett. 35, 247 (2014).
19) I. C. Kizilyalli, A. P. Edwards, O. Aktas, T. Prunty, and D. Bour, IEEE Trans. Electron Devices 62, 414 (2015).
20) A. M. Ozbek and B. J. Baliga, IEEE Electron Device Lett. 32, 300 (2011).
21) O. Aktas and I. C. Kizilyalli, IEEE Electron Device Lett. 36, 890 (2015).
22) T. Kachi and T. Uesugi, Sensors Mater., 25, 3, 219 (2013).
23) I. C. Kizilyalli, P. B. Quanga, D. Disney, H. Bhatia, and Ozgur Aktas, Microelectronics Reliability, 55, 1654 (2015).
24) T. Hayashida, T. Nanjo, A. Furukawa, and M. Yamamuka, Appl. Phys. Exp. 10, 061003 (2017).
25) Z. Hu, K. Nomoto, B. Song, M. Zhu, M. Qi, M. Pan, X. Gao, V. Protasenko, D. Jena, and H. G. Xing, Appl. Phys. Let. 107, 243501 (2015).
26) H. Ohta, K. Hayashi, T. Nakamura, and T. Mishima, 2017 International Meeting for Future of Electron Devices, Kansai, IEEE CAT. No. CFP17567-PRT, 54 (2017).
27) H. Ohta, K. Hayashi, F. Horikiri, T. Nakamura, and T. Mishima, Extended Abstracts of the 2017 Ext. Abstr Solid State Devices and Materials, Sendai, 2017, 671 (2017).
28) Y. Oshima, T. Eri, M. Shibata, H. Sunakawa, K. Kobayashi, T. Ichihashi, and A. Usui, Jpn. J. Appl. Phys. 42, L1-L3 (2003).
29) T. Yoshida, Y. Oshima, T. Eri, K. Ikeda, S. Yamamoto, K. Watanabe, M. Shibata, and T. Mishima, J. Cryst. Growth 310, 5 (2008).
30) B. J. Baliga, Fundamentals of Power Semiconductor Devices. Heidelberg, Germany, Springer-Verlag, 2011.